Magnetic properties on the surface of FeAl stripes induced by nanosecond pulsed laser irradiation

H. Kaiju, Y. Yoshida, S. Watanabe, K. Kondo, A. Ishibashi, and K. Yoshimi

Citation: Journal of Applied Physics **115**, 17B901 (2014); doi: 10.1063/1.4862376
View online: http://dx.doi.org/10.1063/1.4862376
View Table of Contents: http://scitation.aip.org/content/aip/journal/jap/115/17?ver=pdfcov
Published by the AIP Publishing

Magnetic properties on the surface of FeAl stripes induced by nanosecond pulsed laser irradiation

H. Kaiju,[1,a)] Y. Yoshida,[2,3] S. Watanabe,[2] K. Kondo,[1] A. Ishibashi,[1] and K. Yoshimi[4]
[1]*Laboratory of Nano-Structure Physics, Research Institute for Electronic Science, Hokkaido University, Sapporo, Hokkaido 001-0020, Japan*
[2]*Center for Advanced Research of Energy and Materials, Faculty of Engineering, Hokkaido University, Sapporo, Hokkaido 060-8628, Japan*
[3]*Creative Research Institution Sousei, Hokkaido University, Sapporo, Hokkaido 001-0021, Japan*
[4]*Graduate School of Engineering, Tohoku University, Sendai, Miyagi 980-8579, Japan*

(Presented 7 November 2013; received 9 September 2013; accepted 20 October 2013; published online 17 January 2014)

We demonstrate the formation of magnetic nanostripes on the surface of $Fe_{52}Al_{48}$ induced by nanosecond pulsed laser irradiation and investigate their magnetic properties. The magnetic stripe consists of a disordered A2 phase of Fe-Al alloys with Al-oxide along the [110] direction on the (111)-oriented plane. According to the focused magneto-optical Kerr effect measurement, the coercive force of the magnetic stripe obeys the $1/\cos\theta$ law, where θ is the field rotation angle estimated from the stripe direction. Also, the jump field can be observed in the magnetic hysteresis loop. These results indicate that the magnetization reversal in the magnetic stripe originates from the domain pinning, showing that the magnetization rotates incoherently. © *2014 AIP Publishing LLC*. [http://dx.doi.org/10.1063/1.4862376]

Magnetic nanostructures have attracted interest due to the enhancement in magnetic properties. Typically, it is well known that the increase in coercive forces and saturation fields has been observed in magnetic nanostructures, such as nanodots, nanostripes, and nanowires,[1–3] and their behaviors are significantly different from those in the bulk. The mechanism of the magnetization reversal is also strongly related to the dimension and/or shape in nanostructures.[4–7] Moreover, magnetic nanostructures have potential application in bit patterned media (BPM), domain-wall (DW) logic devices, magnetic random access memories (MRAMs), and other functional magnetic devices/materials. Conventional methods for the fabrication of such magnetic nanostructures include lithographic techniques, such as optical, electron-beam, and nanoimprinting lithography, and other methods such as shadow mask, ion irradiation, and self-assembled techniques.[1–3,7–10] Recently, we have proposed laser techniques for the formation of nanostructures.[11,12] In this method, unique nanostructure patterns can be formed due to the self-organization using pulsed laser irradiation. For example, Au/Si nanocomposite structures with uniformly shaped stripe patterns have been produced on a Si(100) surface by pulsed laser irradiation.[11] Also, periodic stripes, polygonal networks, and dot-like nanoprotrusions patterns have been found on the surface of an iron-aluminum (Fe-Al) alloy using the same method.[12] Interestingly, in this system, the magnetic transition from paramagnetism to ferromagnetism can be observed. In this study, we demonstrate the formation of magnetic nanostripes on the surface of $Fe_{52}Al_{48}$ induced by nanosecond pulsed laser irradiation and investigate their magnetic properties, in which we especially focus on the field rotation dependence of the surface magnetization and the mechanism of the magnetization reversal.

Fe-Al alloy button ingots with Al concentration of 48% were prepared using an arc-melting technique in an argon gas atmosphere. The Fe-Al alloy was synthesized as a polycrystalline alloy of ordered B2 phase ($Fe_{52}Al_{48}$). The surface of $Fe_{52}Al_{48}$ was polished to a mirror finish for laser irradiation. The specimens were ultrasonically cleaned and then subjected to pulsed laser irradiation. The $Fe_{52}Al_{48}$ surface was irradiated in air with an Nd:YAG pulse laser (Continuum co., Ltd., Inlite II) at a wavelength of 532 nm, a repetition frequency of 2 Hz, and a pulse width of 5–7 ns at room temperature. The laser irradiation time was 100 s, which corresponds to the laser irradiation with 200 pulses. The laser beam diameter was 6 mm and the irradiation was performed normal to the surface with linearly polarized light having an average laser energy density of 1.24 kJ/m^2.

The surface morphologies of the specimens were observed using a scanning electron microscope (SEM; JEOL, JSM-7001F) and atomic force microscope (AFM; SII NanoTechnology, Nanonavi IIs). The crystalline orientation was examined by the energy backscattering diffraction pattern. Microstructural and microchemical analyses were performed using a transmission electron microscope (TEM; JEOL, JEM-2010F) and an energy-dispersive X-ray spectroscopy (EDS: Noran Vantage) system. The thin foil specimens for TEM observation were prepared using a focused ion beam system. The magnetization curves were measured by focused longitudinal magneto-optical Kerr effect (MOKE) equipment (NEOARK, BH-PI920-HU) under a magnetic field of up to 1 kOe at room temperature. The spot size was set to 3 μm for the observation of the focused MOKE signal.

Figures 1(a) and 1(b) show the SEM images of the (111)-oriented plane of $Fe_{52}Al_{48}$ before and after irradiation, respectively. The surface on $Fe_{52}Al_{48}$ is found to be flat before irradiation, as shown in Fig. 1(a). In contrast, the stripe pattern can be observed along the [110] direction

a)Electronic mail: kaiju@es.hokudai.ac.jp.

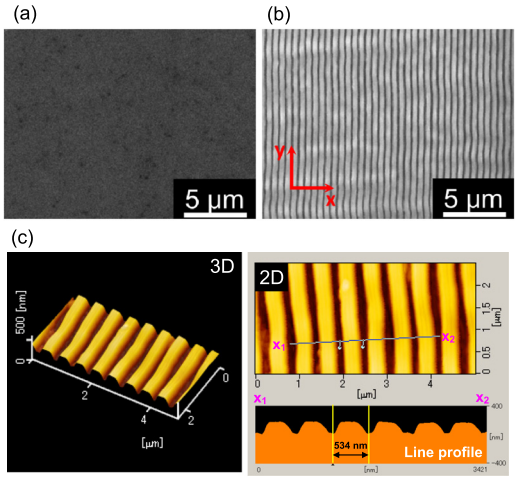

FIG. 1. SEM images of the (111)-oriented plane of $Fe_{52}Al_{48}$ (a) before and (b) after irradiation, respectively. (c) AFM images of the stripe pattern after irradiation.

(y-direction) on the (111)-oriented plane after irradiation in Fig. 1(b).[12] The area of the observed stripe patterns is about 200 μm^2, which corresponds to the size of grains with the (111) surface. Figure 1(c) shows the surface AFM image of $Fe_{52}Al_{48}$ after irradiation. The stripe pattern can be clearly observed from the three-dimensional (3D) plot and the stripe period is found to be an average of 534 nm, which is almost equivalent to the incident laser wavelength, from the line profile and two-dimensional (2D) plot. The stripe height is an average of 155 nm and the width is an average of 242 nm.

Figure 2(a) shows the SEM-EDS mapping of the stripe pattern. From the mapping of Fe and Al indicated by the red and blue images, respectively, their concentrations distribute uniformly in the stripe pattern. In comparison, from the mapping of oxygen (O) indicated by the yellow image, it is confirmed that the aligned oxide exists along the longitudinal direction of the stripe pattern. Figure 2(b) shows the cross-sectional TEM image of $Fe_{52}Al_{48}$ after irradiation along the x-direction illustrated in Fig. 1(b). According to the diffraction patterns and TEM-EDS analyses, the surface of $Fe_{52}Al_{48}$ transforms from the ordered B2 phase to disordered A2 phase with Al-oxide as shown in Fig. 2(c). The transformation from the B2 to A2 phase has been already reported.[12] Here, we find the formation of Al-oxide on the slope of the stripe. Figure 2(d) shows the TEM-EDS result at the point given by the green arrow in Fig. 2(b). From this figure, the strong peaks of Al and O can be observed. The result suggests that Al and O aggregate on the slope of the stripe structure due to the self-organization during pulsed laser irradiation and it is considered that this aggregation gives rise to the formation of Al-oxide.

Figure 3(a) shows the magnetization curves of the (111)-oriented plane of $Fe_{52}Al_{48}$ before and after irradiation, respectively. The magnetic field is applied in the [110] direction, as shown in Fig. 3(a). Before irradiation, the Kerr

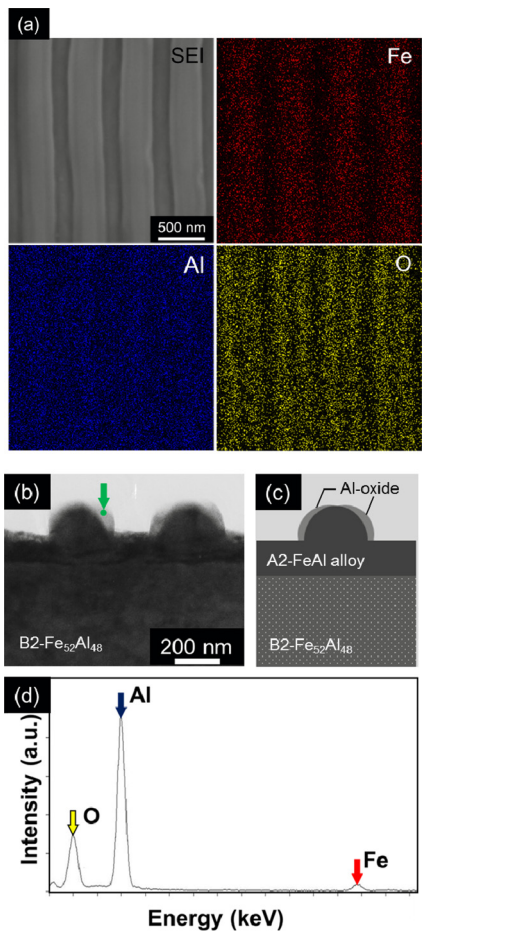

FIG. 2. (a) SEM-EDS mapping after irradiation. (b) Cross-sectional TEM image and (c) schematic illustration of the internal structure for $Fe_{52}Al_{48}$ after irradiation along the x-direction illustrated in Fig. 1(b). (d) EDS at the point given by the green arrow in Fig. 2(b).

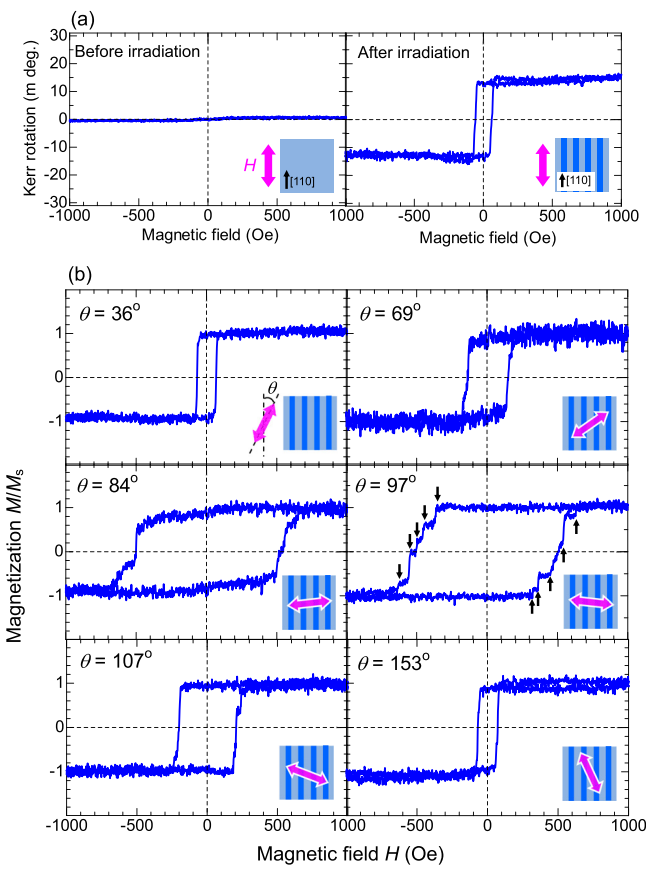

FIG. 3. (a) Magnetization curves of the (111)-oriented plane of $Fe_{52}Al_{48}$ before and after irradiation, respectively. (b) Field rotation dependence of the magnetization curves for the stripe pattern of $Fe_{52}Al_{48}$ after irradiation.

rotation is nearly 0° and there is no coercive force. This behavior indicates paramagnetism, which has been already confirmed as being characteristic of B2-$Fe_{52}Al_{48}$. In comparison, a magnetic hysteresis loop can be measured after irradiation. This magnetization curve exhibits typical ferromagnetic behavior, which is consistent with the structural analysis results that the surface of $Fe_{52}Al_{48}$ becomes the disordered A2 phase, showing ferromagnetism.[9]

Figure 3(b) shows the field rotation dependence of the magnetization curves for the stripe pattern of $Fe_{52}Al_{48}$ after irradiation. Here, the field rotation angle θ is defined by the angle between the applied field and the longitudinal direction of the stripe pattern. From this figure, the coercive force H_c drastically increases up to around 500 Oe as the field rotation angle θ approaches 90°. Figure 4 shows the coercive force as a function of the field rotation angle. The solid circles represent experimental data, and the solid and broken lines represent the calculation results obtained from the DW motion model and Stoner-Wohlfarth (SW) model, respectively. In the DW motion model, the coercive force H_c is given by $H_{c0}/|\cos\theta|$ for $0 \le \theta \le 180°$, where H_{c0} is the coercive force at $\theta = 0°$.[1] This means that the magnetization reversal is mainly driven by the component of the magnetic field parallel to the stripe lines. In the SW model, the relation between the field rotation angle θ and the coercive force H_c is expressed by the equation shown in Ref. 13. This means that the magnetization changes by the coherent rotation. As can be seen from Fig. 4, the experimental results show good agreement with the calculation results by the DW motion model. This means that the magnetization reversal originates from the domain wall pinning, indicating that the magnetization rotates incoherently. Here, it should be noted that there have been several experimental results on the magnetization reversal in magnetic stripe patterns.[1,6,14,15] For example, $Ni_{80}Fe_{20}$, Co, or amorphous $Co_{72}Si_{28}$ stripe patterns have the magnetic easy (hard) axis in the direction parallel (perpendicular) to the stripes due to their strong shape anisotropy.[1,14,15] These magnetization reversals can be explained by the coherent rotation of SW model. As another example, the coercive field for an array of amorphous $Fe_{70}Si_{30}$ lines shows an $H_c \propto 1/\cos\theta$ behavior.[1] This suggests that the magnetization reversal takes place by the DW motion, dominated by the magnetic pinning. In other cases, the transition from curling-mode to coherent-mode or transverse-mode rotation has been observed in Fe_3O_4 or CoCrPt magnetic nanotubes.[16–18] Thus, several mechanisms have been proposed for the magnetization reversal in magnetic stripes or nanotubes. Among them, our experimental results can be explained by the DW motion model, which is similar to the magnetization reversal in amorphous $Fe_{70}Si_{30}$ stripes. Here, note that some "jump" fields H_{jump} can be observed in Fig. 3(b). Typically, the "jump" fields H_{jump}, indicated by arrows in Fig. 3(b), can be seen in the magnetic field $|H|$ of 300–600 Oe for $\theta = 97°$. This result is surely consistent with the fact that the magnetization reversal mechanism is incoherent, i.e., that domain structures mediate the jump process.[6] Also, according to the structural analysis, Al-oxide is

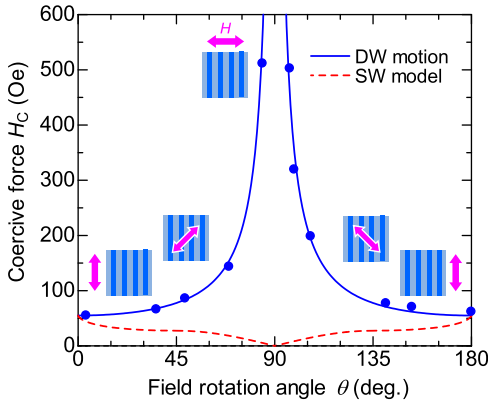

FIG. 4. Coercive force as a function of the field rotation angle for the stripe pattern of $Fe_{52}Al_{48}$ after irradiation. The solid circles represent experimental data and the solid and broken lines represent the calculation results obtained from the DW motion model and SW model, respectively.

confirmed on the slope of stripes from Fig. 2. This Al-oxide is considered to act as a magnetic pinning site. We conclude that the magnetization reversal in Fe-Al magnetic stripes formed by nanosecond pulsed laser irradiation originates from the domain wall pinning. Thus, the nanosecond pulsed laser technique can serve as a powerful tool for obtaining magnetic nanostructures. Moreover, as mentioned in the Introduction, nanodot patterns can be fabricated using this technique. In nanodot patterns, an increase of H_c can be expected since the small dimension of dots impedes the formation of magnetic multi-domain structures. Therefore, this technique will also open up new opportunities for the production of high-H_c materials and the magnetic storage application.

This research has been partially supported by the Management Expenses Grants for National Universities Corporations and "Nanotechnology Platform" Program from The Ministry of Education, Culture, Sports, Science and Technology (MEXT) and Precursory Research for Embryonic Science and Technology program from Japan Science and Technology Agency (JST). The authors would like to express their sincere appreciation to O. Kitakami of Tohoku University for his helpful discussion.

[1]J. I. Martín *et al.*, J. Magn. Magn. Mater. **249**, 156 (2002).
[2]W. C. Uhlig and J. Shi, Appl. Phys. Lett. **84**, 759 (2004).
[3]R. K. Dumas *et al.*, Phys. Rev. B **75**, 134405 (2007).
[4]E. H. Frei *et al.*, Phys. Rev. **106**, 446 (1957).
[5]J. F. Smyth *et al.*, J. Appl. Phys. **69**, 5262 (1991).
[6]A. O. Adeyeye *et al.*, Phys. Rev. B **56**, 3265 (1997).
[7]K. Liu *et al.*, Appl. Phys. Lett. **81**, 4434 (2002).
[8]C. Chappert *et al.*, Science **280**, 1919 (1998).
[9]E. Menéndez *et al.*, Small **5**, 229 (2009).
[10]D. Oshima *et al.*, IEEE Trans. Magn. **49**, 3608 (2013).
[11]Y. Yoshida *et al.*, Nanotechnology **22**, 375607 (2011).
[12]Y. Yoshida *et al.*, Appl. Phys. Lett. **102**, 183109 (2013).
[13]E. C. Stoner and E. P. Wohlfarth, Trans. R. Soc. A **240**, 599 (1948).
[14]S. P. Li *et al.*, Appl. Phys. Lett. **77**, 2743 (2000).
[15]J. G. S. Duque *et al.*, J. Phys. D: Appl. Phys. **43**, 025001 (2010).
[16]J. Escrig *et al.*, Nanotechnology **18**, 445706 (2007).
[17]S. Shamaila *et al.*, Appl. Phys. Lett. **94**, 203101 (2009).
[18]O. Albrecht *et al.*, J. Appl. Phys. **109**, 093910 (2011).